

The Preparation and Microstructure of Semi-Solid 7075 Alloy Slurry

G.-S. GAN^a, B. YANG^{a,b,*}, S.-Y. BEI^a AND H. MEI^a

^aState Key Laboratory for Advanced Metals and Materials, University of Science & Technology Beijing
Beijing 100083, China

^bInternational Centre for Materials Physics, Chinese Academy of Sciences, Shenyang, 110016, China

A novel technique, with which *in situ* TiB₂ particles and serpentine channels are introduced to prepare wrought aluminum alloy with higher strength, has been successfully applied to produce semi-solid 7075 alloy slurry. The effects of *in situ* TiB₂ particles and serpentine channels on the microstructure of the 7075 alloy including the grain growth behavior in the semi-solid state of the 7075 alloy were investigated. The experimental results showed that the *in situ* TiB₂ particles and serpentine channels are beneficial to increase the number of solidification nuclei and to promote uniform distribution of α -Al nuclei. As a result, the semi-solid 7075 alloy slurry with globular-like grains has been successfully produced.

PACS: 81.05.Bx, 82.40.-g, 98.20.Gm

1. Introduction

Investigations over the past four decades have shown that semi-solid metal (SSM) processing can be readily utilized to synthesize aluminum alloys, especially for traditional casting aluminum alloys, such as A356 and A357 alloys. Recently, the development of SSM for manufacturing wrought aluminum alloys with higher strength has attracted considerable interest [1–3]. Compared with traditional casting aluminum alloys, however, the change of solid fraction as a function of temperature for wrought aluminum alloys is too sensitive to produce semi-solid wrought aluminum alloys slurries [4, 5]. On the other hand, semi-solid alloys slurries are known to be stirred in order to destroy or hinder the formation of dendrite grains. Unfortunately, it is not easy to stir the wrought aluminum alloys due to the fact that the dendrite-like grains of these alloys are fairly developed during their solidification process. According to the authors' knowledge, little is known about the preparation of wrought aluminum alloy slurries [6].

More recently, the present authors have developed a novel technique [7]. In this technique, a matrix alloy is melted firstly, and then the reinforcements are *in situ* synthesized in the molten alloy by chemical reactions between the elements or between the elements and the ceramic compounds. Our previous results have showed that the *in situ* Al₂O₃, TiC, TiB₂ particles not only can improve the strength and modulus of aluminum alloys due to higher hardness and modulus of the particles, but

also can refine effectively the grains of the aluminum alloys [8]. It is noteworthy that these particles formed by *in situ* synthesis can also retard the grain growth of an alloy when the alloy is heated in its solid–liquid phase region [9]. This work focuses on the effects of *in situ* TiB₂ particles and serpentine channels on the microstructure of the 7075 wrought aluminum alloy. The use of serpentine channels has an advantage because they are relatively simple and can increase effectively the number of α -Al nuclei.

2. Experimental

The composition of 7075 alloy used in this research is presented in Table. First, the 7075 wrought aluminum alloy was melted and heated up to 850 °C, after which a mixture of K₂TiF₆ and KBF₄ was added to the molten 7075 aluminum alloy at a Ti–B molar ratio of 1:2. When all reactions were completed (the end point of the reaction can be determined after observing the dazzling blue light originating from the reacted K₂TiF₆ and KBF₄ mixture), the melt was degassed by using C₂Cl₆ at 720 °C. Then the molten 7075 alloy and 3%TiB₂/7075 composite (the mass%, all the same below) were poured and flowed through one or two serpentine graphite channels preheated at two different temperatures, 300 and 600 °C. The diameter of the serpentine graphite channel is 20 mm. The lengths of one and two serpentine graphite channels are the same, i.e. 390 mm in order to elucidate the effect of curve number in the serpentine channels on the grain size of the 7075 alloy and 3%TiB₂/7075 composite. Finally, the slurries were quenched in a stainless

* corresponding author; e-mail: byang@ustb.edu.cn

steel beaker with a size of $\phi 50 \times 2 \times 70$ mm³. The stainless steel beaker was cooled in adequate water.

TABLE
Chemical composition (wt%) of the 7075 Al alloy.

Zn	Mg	Cu	Si	Fe	Mn	Cr	Ti	Al
5.52	2.36	1.51	0.18	0.26	0.15	0.25	0.03	balance

The liquidus and solidus temperatures of the alloy were tested by NETZSCH DSC204 differential scanning calorimetry (DSC) with a heating rate of 10 °C/min. The specimens of the 7075 alloy and 3%TiB₂/7075 composite were etched in a solution of mixed acids (2 ml HF + 3 ml HCl + 5 ml HNO₄ + 250 ml H₂O). The microstructures of 7075 alloy and 3%TiB₂/7075 composite were examined using optical microscope (OM) and ZEISS SUPRA 55 Field Emission Gun scanning electron microscopes.

3. Results and discussion

3.1. The preparation of semi-solid 7075 alloy slurry

Figure 1a shows the DSC curve of the 7075 alloy. One can see that the gap between the liquidus and solidus temperature of the alloy is about 162 °C. Figure 1b shows a typical micrograph of the alloy, which is mainly composed of dendrite-like grains. The liquid fraction of the 7075 alloy as a function of temperature in its solid–liquid phase region was calculated and shown in Fig. 1c, showing that the liquid fraction of the alloy is too sensitive to produce semi-solid slurry.

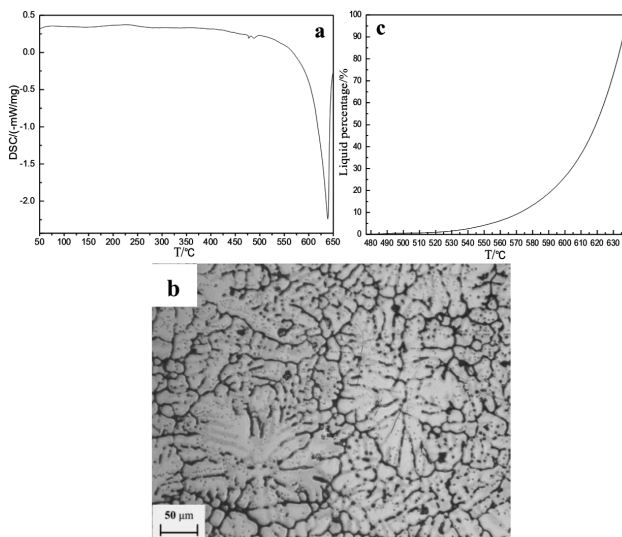


Fig. 1. The DSC curve (a), the microstructure (b) and the liquid percentage as a function of temperature during the solid–liquid phase region for the 7075 alloy (c).

Figure 2 shows the microstructure of the semi-solid 7075 alloy after flowing through one serpentine graphite

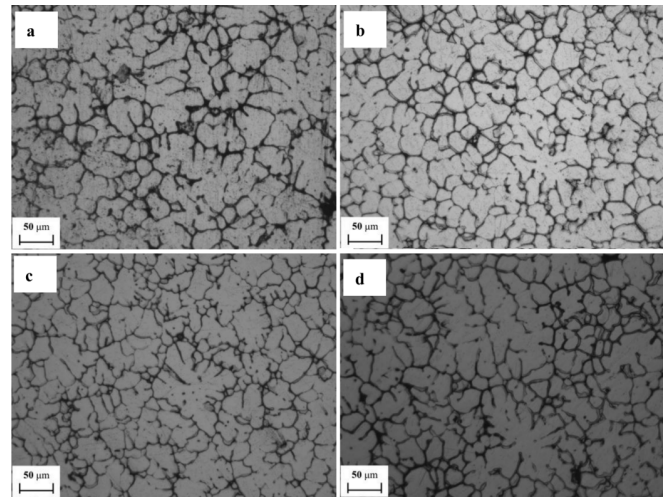


Fig. 2. The microstructures of semi-solid 7075 alloy after the molten alloy flowed through one serpentine graphite channel without preheating (a, b) and preheated at 300 °C (c, d). The pouring temperatures are 685 °C (a, c) and 670 °C (b, d), respectively.

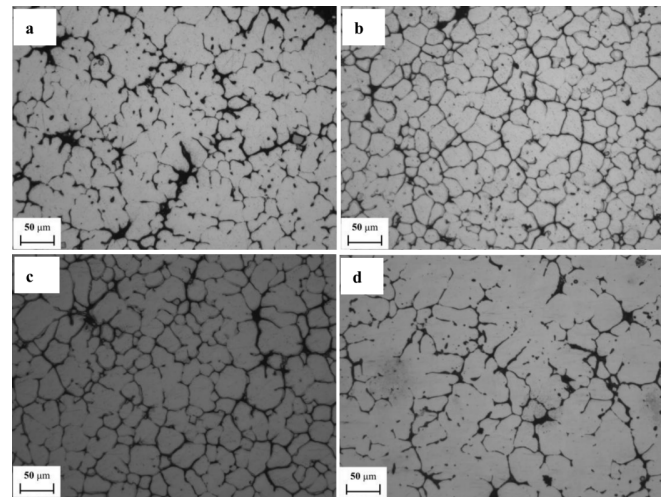


Fig. 3. The microstructures of semi-solid 7075 alloy after the molten alloy flowed through one serpentine graphite channel preheated at 600 °C. The pouring temperatures are 685 °C (a), 670 °C (b), 655 °C (c), and 640 °C (d), respectively.

channel without preheating and preheated at 300 °C, respectively. The pouring temperatures are 685 °C and 670 °C, respectively. One can see that the 7075 Al alloy is mainly composed of dendrite-like grains when poured at 685 °C, as shown in Fig. 2a,c. The dendrite-like grains become rose-like ones with decreasing of the pouring temperature, as shown in Fig. 2b. With increasing of the preheating temperature of the serpentine graphite channel, its cooling capacity decreases and thus the grains of the 7075 alloy become coarser, as shown in Fig. 2d.

Figure 3 shows the microstructure of semi-solid 7075 alloy when the molten alloy flows through one serpentine

graphite channel preheated at 600 °C. One can see that some larger dendrite-like grains exist in the alloy when poured at 685 °C, as shown in Fig. 3a. With decreasing of the pouring temperature from 685 °C to 670 °C, the dendrite-like grains change gradually to rose-like ones, as shown in Fig. 3b. However, the rose-like grains in this case grow again to the dendrite-like ones with decreasing the pouring temperature to 655 °C, as shown in Fig. 3d. Anyway, no fine globular grains can be formed in the cases mentioned above.

3.2. The preparation of semi-solid 3%TiB₂/7075 composite slurry

The possible reaction to form TiB₂ in the molten 7075 alloy fabricated by this technique can be expressed as [10]

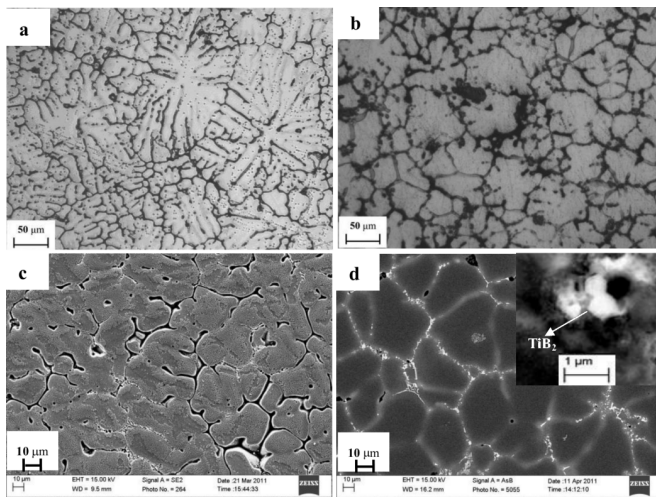


Fig. 4. The microstructures of 7075 alloy and 3%TiB₂/7075 composite after pouring into graphite mould at the pouring temperature of 720 °C: 7075 alloy (a), (c), 3%TiB₂/7075 composite (b), (d).

According to Eq. (1), KF and AlF₃ can be easily eliminated from the dregs. Figure 4 shows the microstructures of 7075 alloy and 3%TiB₂/7075 composite after pouring into graphite mould at room temperature. We can see that the 7075 alloy is mainly composed of dendrite-like grains. In this case, the maximum grain size of the alloy is about 250 μm. After *in situ* adding of 3%TiB₂ particles in the alloy, the grains of the alloy were refined effectively. The maximum grain size of the composite is about 150 μm. In order to study further the distribution of the TiB₂ particles, a higher resolution image of the 3%TiB₂/7075 composite was obtained by means of SEM, as shown in Fig. 4d. It can be seen that the *in situ* TiB₂ particles (bright phases) are agglomerated at the grain boundary of the α-Al phase. The morphologies of the TiB₂ particles are hexagonal-like, and the mean size

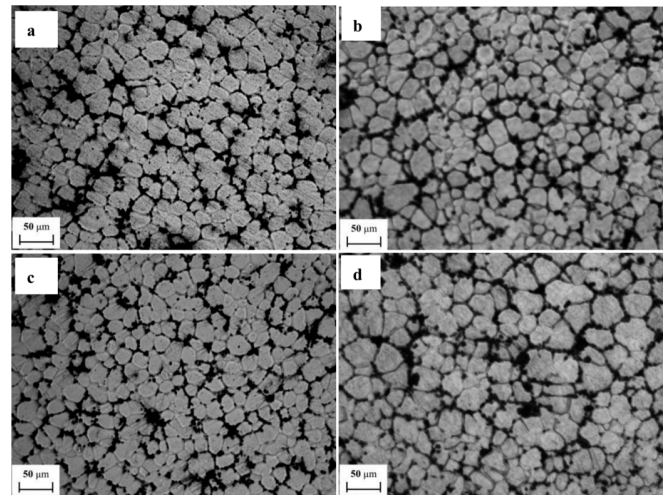


Fig. 5. The microstructures of semi-solid 3%TiB₂/7075 composite after the molten composite flowed through one serpentine graphite channel preheated at 600 °C. The pouring temperatures are 685 °C (a), 670 °C (b), 655 °C (c), and 640 °C (d), respectively.

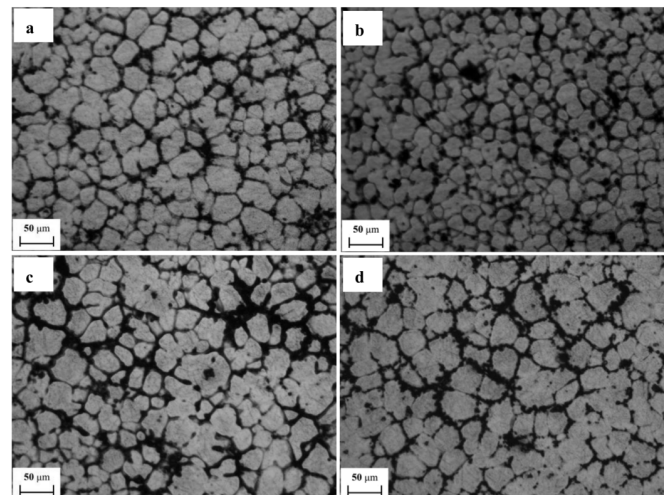


Fig. 6. The microstructures of semi-solid 3%TiB₂/7075 composite after the molten composite flowed through two serpentine graphite channels preheated at 600 °C. The pouring temperatures are 685 °C (a), 670 °C (b), 655 °C (c), and 640 °C (d), respectively.

of the TiB₂ particles is about 500 nm, as shown in the inset in Fig. 4d.

Figure 5 shows the microstructure of the semi-solid TiB₂/7075 composite when the molten composite flows through one serpentine graphite channel preheated at 600 °C. One can see that the mean grain sizes of the alloy reduce to 25 and 23 μm at 670 °C and 655 °C pouring temperatures, respectively.

Figure 6 shows the microstructure of semi-solid 3%TiB₂/7075 composite flowed through two serpentine graphite channels when preheated at 600 °C. Fine glob-

ular grains can be got and the mean grain sizes of the composite are 29 and 26 μm at 685 °C and 670 °C pouring temperatures, respectively. However, the grain of the composite grows up to 38 μm when pouring temperature decreases to 655°.

As mentioned previously, the TiB_2 particles are mostly with a hexagonal-like and with a mean size of 500 nm, as shown in Fig. 4d. The reasons why the TiB_2 particles and serpentine graphite channels can effectively refine the α -Al phase may be attributed to the following factors. First, the presence of TiB_2 particles increases the nucleation kinetics of the α -Al phase by increasing the density of nuclei in the melt, which is beneficial to the formation of fine α -Al phase. Second, the surface-active TiB_2 particles are pushed onto the solid/liquid interface front and enriched at the α -Al boundaries during solidification, which obstruct solute redistribution and refine the α -Al phase. Third, the fine globular grains formed on the well of serpentine graphite channel during pouring process can be easily taken off by the molten fluid of the composite and flow into the molten composite, which increase number of solidification nuclei and are beneficial to promote uniform distribution of α -Al nuclei.

4. Conclusions

(1) A novel semi-solid metal processing technique, with which *in situ* TiB_2 particles and serpentine channel are introduced to prepare 7075 wrought aluminum alloy, has been successfully applied to produce semi-solid 7075 alloy slurry.

(2) The *in situ* TiB_2 particles and serpentine channel

are beneficial to increase number of solidification nuclei and to promote uniform distribution of α -Al nuclei.

Acknowledgments

This work was supported by the National High Technology Research and Development Program ("863"Program) of China under No. 2009AA03Z523.

References

- [1] U.A. Curle, G. Govender, *Trans. Nonferrous Met. Soc. China* **20**, 832 (2010).
- [2] S.P. Midson, *Die Casting Eng.* **50**, 48 (2006).
- [3] H.V. Atkinson, P. Kapranos, in: *Proc. Sixth Int. Conf. on Semi-Solid Processing of Alloys and Composites*, Eds. G.L. Chiarmetta, M. Rosso, Unione Industriale di Torino, Turin 2000, p. 443.
- [4] H. Kaufmann, H. Wabusseg, *Aluminum* **76**, 70 (2000).
- [5] G. Vaneetveld, A. Rassili, *Diff. Def. Data Part B: Solid State Phenomena* **141-143**, 707 (2008).
- [6] S. Chayong, P. Kapranos, H.V. Atkinson, in Ref. [3], p. 649.
- [7] B. Yang, W. Feng, J.S. Zhang, *Acta Mater.* **51**, 4977 (2003).
- [8] B. Yang, G.S. Gan, H.B. Zhang, Z.Z. Fang, *Mater. Sci. Eng. A* **528**, 5649 (2011).
- [9] L. Zhang, G.S. Gan, B. Yang, *Mater. Trans.* **52**, 1646 (2011).
- [10] C. Tjong, Z.Y. Ma, *Mater. Sci. Eng. A* **29**, 49 (2000).